

## Interplay between long-range elastic and short-range chemical interactions in Fe-C martensite formation

A. Udyansky,<sup>1</sup> J. von Pezold,<sup>1</sup> V. N. Bugaev,<sup>2</sup> M. Friák,<sup>1</sup> and J. Neugebauer<sup>1</sup>

<sup>1</sup>Max-Planck-Institut für Eisenforschung GmbH, Max-Planck-Straße 1, D-40237 Düsseldorf, Germany

<sup>2</sup>Max-Planck-Institut für Metallforschung, Heisenbergstraße 3, D-70569 Stuttgart, Germany

(Received 9 March 2009; revised manuscript received 6 May 2009; published 17 June 2009)

The thermodynamic stability of tetragonal and cubic states of dilute Fe-C interstitial solid solutions is studied combining atomistic simulations with the microscopic elasticity theory. This approach allows us to accurately describe the effect of long-ranged elastic C-C interactions on the martensite formation. The predicted compositional dependence of the critical temperature at which the cubic phase transforms into tetragonal states is in good agreement with available experimental data and thus removes previous controversies regarding the relative importance of strain-induced and chemical interactions.

DOI: [10.1103/PhysRevB.79.224112](https://doi.org/10.1103/PhysRevB.79.224112)

PACS number(s): 61.66.Dk, 05.50.+q, 64.60.Cn, 61.72.-y

### I. INTRODUCTION

Mechanical properties of steels can vary tremendously depending on chemical composition and thermomechanical treatments. The body-centered-cubic (bcc) tetragonally distorted states of interstitial Fe-C solid solutions are known as martensite,<sup>1,2</sup> a metastable product obtained by quenching the high-temperature austenitic [face-centered-cubic (fcc)] phase. Martensitic transformation is not only the mechanism behind steel strengthening but also the origin of unusual mechanical properties such as reversible strain, superelasticity, superplasticity, and high mechanical damping.<sup>3</sup>

The linear concentration dependence of the lattice parameters and the tetragonality of martensitic Fe-C solid solutions<sup>4,5</sup> are linked to the martensitic Bain's transformation occurring via diffusionless atomic rearrangements<sup>6,7</sup> from the fcc austenite to the bcc ferrite. The change in structure is achieved by homogeneous deformation when the carbon atoms originally occupying octahedral sites within the fcc lattice fall into only one interstitial sublattice of the bcc  $\alpha$ -Fe, which causes a tetragonal distortion of the resulting lattice. Such a preferential distribution of the carbon atoms can be interpreted as orientational ordering. In contrast, if carbon atoms occupy all three sublattices randomly, the resulting lattice is cubic. Diffraction experiments performed on samples exhibiting both relatively low<sup>8</sup> and high<sup>9</sup> tetragonality revealed that at room temperature the ordered distribution of the carbon atoms is thermodynamically more advantageous than the disordered one due to the interactions between carbon atoms.

A strong focus of previous theoretical studies was on the compositional dependence of the critical temperature at which the ordered tetragonal states become thermodynamically more stable than the disordered cubic ones. Zener<sup>10</sup> suggested that the elastic (strain-induced) interactions between carbon impurity atoms result in their preferential distribution over a single sublattice of octahedral interstices in bcc Fe and, consequently, a tetragonal state. Kurdjumov and Khachatryan<sup>11-13</sup> developed a theoretical approach to describe the order-disorder transition using the static concentration waves method<sup>13</sup> and microscopic elasticity theory (MET).<sup>13-16</sup> The MET has been developed to describe long-

range strain-induced interactions between point defects in an alloy matrix. It is formulated in  $\mathbf{k}$  space and does not *a priori* limit the radius of interactions. Input parameters for the MET are Kanzaki forces<sup>17</sup> acting on the host matrix in the presence of impurity atoms and components of the Born-von-Karman tensor<sup>18</sup> describing the interatomic interactions within the host lattice. Kanzaki forces can be regarded as a virtual force field acting on the atoms of the ideal (i.e., impurity free) host lattice to imitate the real atomic displacements in the presence of an impurity atom. In an atomistic calculation, they can be easily computed by removing the interstitial C atom but keeping the relaxed host atoms fixed. The Kanzaki forces are then simply the forces acting on the displaced host atoms. Note that the MET is rigorously defined for interstitial alloys since they can be strictly separated into a metal matrix and an impurity subsystem.

Within the MET, which describes strain-induced interactions only, the critical concentration at room temperature has been predicted.<sup>10,12,19-22</sup> However, it has been shown<sup>23</sup> that the elastic interactions by themselves cannot account for the stability of the tetragonal phase in Fe-C solid solutions and the chemical C-C interactions also have to be considered<sup>13</sup> in order to properly describe the martensitic transformation. Using this approach, a critical C concentration of 0.03 wt % at room temperature has been determined,<sup>13</sup> which is substantially lower than the recently found experimental value of 0.18 wt %.<sup>24</sup> This discrepancy may be due to the inadequate description of the chemical C-C interactions within the Fe matrix by the interaction potential, which had been parametrized to C-C interactions in organic crystals.

In this paper, we address the problem of martensitic stability limits in dilute Fe-C solid solutions using a combination of the MET and atomistic potentials. This combined approach allows for a consistent description of the strain-induced and the chemical part with all parameters determined from the atomistic simulations. The relative importance of these two contributions to the interaction energy can thus be directly examined and the order/disorder transformation may be described.

### II. METHOD

The atomistic determination of the C-C interactions within the Fe-C system was performed using the embedded

TABLE I. Parameters for the determination of the Kanzaki forces and the dynamical matrix obtained using atomistic (EAM) simulations, as compared to experimental values. Elastic constants are in GPa, lattice constant in Å.

Method	$a_0$	$c_{11}$	$c_{12}$	$c_{44}$	$L_{xx}$	$L_{zz}$
EAM	2.867	242	137	122	-0.12	0.84
Exp.	2.861 <sup>30</sup>	243 <sup>31</sup>	138 <sup>31</sup>	122 <sup>31</sup>	-0.09 <sup>30</sup>	0.86 <sup>30</sup>

atom method (EAM) implemented in the IMD code.<sup>25</sup> The EAM interaction potential<sup>26</sup> has been fitted to experimentally measured crystal properties of the perfect crystal (lattice parameters and elastic constants) as well as to energies and configurations of point defects and clusters predicted by density-functional theory. Despite the known limitations of Finnis-Sinclair-type potentials in accurately reproducing, e.g., energies and structures of self-interstitials and screw dislocations in iron, the potential used has been carefully checked to reproduce all quantities relevant for this study. The elastic constants and lattice parameters of bulk bcc Fe as well as the dependence of the lattice constants on the interstitial C concentration are close to their corresponding experimental values (see Table I). Moreover, the lattice distortions around a C interstitial in the octahedral site closely match the predictions from previous *ab initio* calculations.<sup>27</sup> The interatomic distance between the impurity atom and first- and second-nearest neighbors is increased by 22.9% and decreased by 1.94%, respectively (*ab initio*:<sup>27</sup> +24.3%, -1.8%; experiment:<sup>28</sup> +38%, -2.6%). Finally, the relative stability of octahedral and tetrahedral sites as well as C-C binding energies within the Fe matrix determined using this potential are in agreement with previous *ab initio* results.<sup>26,27</sup>

Using this potential, the *chemical* contribution to the interatomic interaction as a function of the C-C distance,  $\rho$ , was determined by calculating the energy of the system with all the atoms constrained to their ideal positions. The pairwise chemical interaction was thus determined using

$$V_{\rho}^{\text{ch}} = E_{\rho}^0(\text{Fe} + 2\text{C}) - E(\text{Fe}) - 2\Phi^0, \quad (1)$$

where  $\Phi^0 = E^0(\text{Fe} + 1\text{C}) - E(\text{Fe})$  is the energy of injection of an interstitial C atom into the Fe host,  $E_{\rho}^0(\text{Fe} + 2\text{C})$  and  $E^0(\text{Fe} + 1\text{C})$  are the energies of the systems containing two C atoms separated by a distance  $\rho$  and a single C atom within the Fe matrix, respectively, and  $E(\text{Fe})$  is the energy of the Fe matrix.

The *strain-induced* contribution to the C-C interactions was calculated atomistically by relaxing the Fe matrix, while constraining the interstitial C atoms to their ideal positions separated by  $\rho$ . The corresponding energy expression reads

$$V_{\rho}^{\text{si}} = E_{\rho}^{\text{rel}}(\text{Fe} + 2\text{C}) - E_{\rho}^0(\text{Fe} + 2\text{C}) - 2(\Phi^{\text{rel}} - \Phi^0), \quad (2)$$

where  $E_{\rho}^{\text{rel}}(\text{Fe} + 2\text{C})$  is the energy of the system in the presence of two C atoms and  $\Phi^{\text{rel}}$  is the injection energy of a single C atom after a full geometry optimization.

Both  $V_{\rho}^{\text{ch}}$  and  $V_{\rho}^{\text{si}}$  were determined atomistically using a cubic supercell with periodic boundary conditions consisting

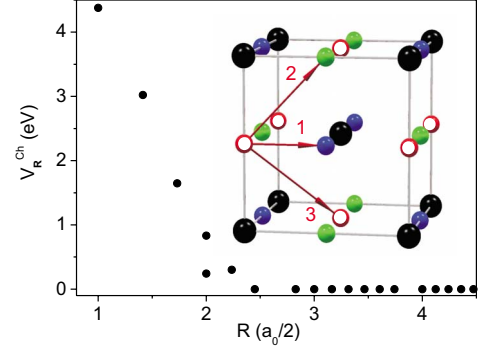


FIG. 1. (Color online) Dependence of the pairwise chemical contribution to the C-C interactions as a function of the C-C distance. The structure of the complex lattice, consisting of three interpenetrating bcc sublattices of octahedral interstices [hollow, green, blue (print: hollow, light gray, dark gray) balls] within the Fe matrix (black balls), is schematically shown in the inset. The first three coordination shells are indicated by arrows.

of 16 000 Fe atoms and two interstitial C atoms in octahedral sites (see inset of Fig. 1).

Within the MET, it is convenient to describe the interaction between two interstitials at positions  $p$  and  $q$  in two unit cells separated by translation vector  $\mathbf{R}$  in matrix form  $\|V_{pq}(\mathbf{R})\|$ .<sup>13</sup> In such a matrix, the diagonal elements correspond to the effective cluster interactions within one sublattice and nondiagonal elements describe the interactions between atoms on different sublattices. The strain-induced contribution in reciprocal space reads<sup>13,14</sup>

$$V_{pq}^{\text{si}}(\mathbf{k}) = -\mathbf{F}_p(\mathbf{k})\mathbf{G}(\mathbf{k})\mathbf{F}_q^*(\mathbf{k}) + Q_{pp}\delta_{pq}, \quad (3)$$

$$Q_{pp} = \frac{1}{N} \sum_{\mathbf{k}} \mathbf{F}_p(\mathbf{k})\mathbf{G}(\mathbf{k})\mathbf{F}_p^*(\mathbf{k}), \quad (4)$$

where the summation is carried out over  $N$  wave vectors  $\mathbf{k}$  in the first Brillouin zone.  $\mathbf{F}_p(\mathbf{k})$  is the Fourier transform of the pairwise Kanzaki force,  $\mathbf{G}(\mathbf{k}) = \mathbf{D}^{-1}(\mathbf{k})$  ( $\mathbf{k} \neq 0$ ) is the Fourier component of the lattice Green's function,<sup>18</sup>  $\mathbf{D}(\mathbf{k})$  is the dynamical matrix,  $\delta_{pq}$  is the Kronecker delta, and  $Q_{pp}$  is introduced in order to exclude self-interaction of interstitial atoms.

The Kanzaki forces  $\mathbf{F}_p(\mathbf{k})$  are determined using an analytical model and depend on the elastic constants  $c_{ij}$ , the lattice constant  $a_0$  of the host matrix in the absence of C interstitials, as well as coefficients  $L_{xx} = \frac{1}{a_x} \frac{da_x}{dc}$  and  $L_{zz} = \frac{1}{a_z} \frac{da_z}{dc}$  (see, e.g., Ref. 29), which describe the concentration dependence of the carbon-induced lattice distortions in the [100] and [001] directions, respectively. The Kanzaki forces were evaluated up to the second-nearest-neighbor shell of the host lattice surrounding the interstitial C atoms.  $\mathbf{G}(\mathbf{k})$  depends on  $c_{ij}$  and  $a_0$  only.

### III. RESULTS

The chemical contribution to the C-C interactions,  $V_{\rho}^{\text{ch}}$ , was determined atomistically as shown in Fig. 1. It is a fast decaying function with a range defined by the cutoff radius

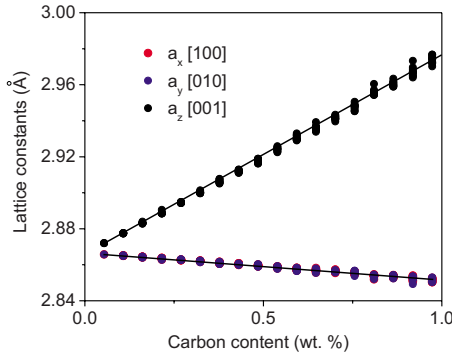


FIG. 2. (Color online) Dependence of the lattice parameters of Fe-C solid solutions on the C concentration using the atomistic EAM simulations. The larger scatter in the obtained lattice parameters at higher concentrations is a result of direct chemical C-C interactions. The solid line is a linear least-squares fit to the calculated data and used to determine the parameters  $L_{xx}$  and  $L_{zz}$ .

of the EAM potential and can thus be parametrized by a small number of effective pair interactions.

The input parameters for the MET as obtained using the EAM potential are summarized in Table I. The equilibrium lattice constant  $a_0$  was found by fitting the Murnaghan equation of state to the total energies of the Fe matrix as a function of the unit-cell volume. The elastic constants  $c_{11}$ ,  $c_{12}$ , and  $c_{44}$  were obtained by computing the energetic response to volume-conserving orthorhombic and monoclinic distortions of the cubic unit cell.

$L_{xx}$  and  $L_{zz}$  were evaluated by calculating the C concentration dependence of the Fe-C lattice constant along the [001], [010], and [001] directions (Fig. 2) using a 2000 atom cubic supercell. The atomic positions and the shape of the supercell were allowed to relax according to the forces and internal strain determined using the EAM potential. For each given concentration C atoms were distributed randomly within one interstitial sublattice of the Fe matrix. In order to remove statistical noise, the lattice parameters obtained from ten randomly generated C distributions have been calculated (dots in Fig. 2) and averaged for each concentration in the least-squares fit.

In order to compare the strain-induced interactions obtained within the MET [in reciprocal space—Eq. (3)] and by atomistic simulations [in real space—Eq. (2)] we use the Fourier transform

$$V_{pq}^{si}(\mathbf{R}) = \frac{1}{N} \sum_{\mathbf{k}} V_{pq}^{si}(\mathbf{k}) e^{i\mathbf{k}\mathbf{R}}. \quad (5)$$

The results are shown in Fig. 3. The qualitative agreement between these two approaches in real space is evident—both strain-induced pair interactions exhibit a similar long-range oscillatory behavior originating from the slow decay of the displacement field. The long-range character of the strain-induced part makes a description in a real-space formulation challenging, while it is naturally taken into account in a reciprocal-space approach (e.g., the MET). The large discrepancy observed for the first two interatomic shells is attributed to the small C-C distances, for which the concept of

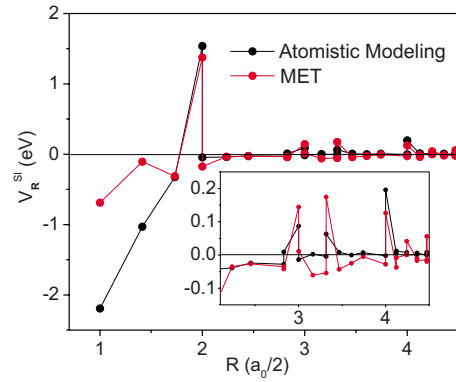


FIG. 3. (Color online) Comparison of the pairwise strain-induced part of the C-C interactions calculated atomistically (black line) and using the MET (red line).

lattice mediated elastic interaction assumed in the MET may not be applicable. Note, that while the Kanzaki forces for the third and higher coordination shells are neglected, the long-range strain-induced interactions are nonetheless well described.

For a more detailed comparison of the atomistic and the MET approach, we analyze the dispersion of the strain-induced interaction  $V_{pq}^{si}(\mathbf{k})$  in reciprocal space. As a typical example, Fig. 4 shows the dispersion for the  $V_{11}(\mathbf{k})$  term of the interaction matrix. Irrespective of the method used to obtain the strain-induced interaction parameters (MET or atomistic simulations), the same trends are observed: the position of the (global) minimum of  $V_{11}^{si}(\mathbf{k})$  in the  $\Gamma$ -H direction is approaching the  $\Gamma$  point as the number of coordination shells taken into account in the Fourier transform is increased. In the limit of an infinite interaction range, the Fourier component of the strain-induced interactions exhibits a nonanalytic behavior: the value of  $V_{11}^{si}(\mathbf{k})$  at the  $\Gamma$  point depends strongly on the direction along which the wave vector  $\mathbf{k}$  approaches  $\Gamma$  but not on the modulus of  $\mathbf{k}$ . The nonanalytic

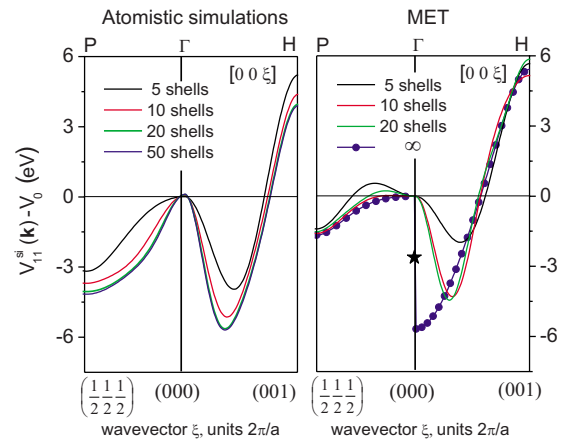


FIG. 4. (Color online) Effect of truncating the interaction radius in real space on the Fourier transform of the strain-induced interactions in the vicinity of the  $\Gamma$  point. The value  $V_{11}^{si}(\mathbf{k}=0) = -\frac{a^3}{2} \{2c_{11}L_{xx}(L_{xx} + 2L_{zz}) + c_{11}(2L_{xx}^2 + L_{zz}^2)\} + Q$  in the continuum limit of the MET (Ref. 13) is indicated by the star. The interactions are referenced to their value,  $V_0$ , at the  $\Gamma$  point in the P- $\Gamma$  direction.

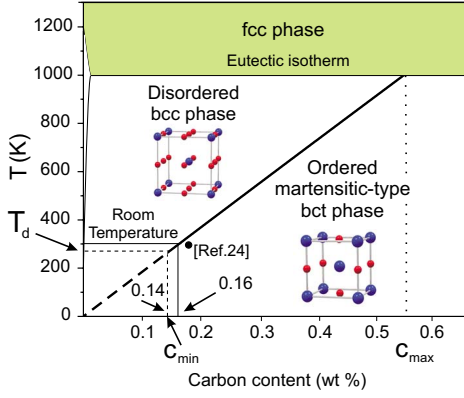


FIG. 5. (Color online) Predicted phase diagram of dilute Fe-C solid solutions. The temperature of absolute stability loss ( $T_c$ ) obtained by our calculations is indicated by the solid black line. The black dot corresponds to the only available experimental data.  $c_{\max}$  is the limiting C concentration above which the disordered phase becomes thermodynamically unstable irrespective of temperature.  $T_d$  defines the temperature below which the structure of the Fe-C solid solution is kinetically controlled due to the slow diffusion of the interstitial C atoms and  $c_{\min}$  indicates the corresponding minimal C concentration below which no martensitic transformation is expected.

ticity is not well described by the atomistic simulations. This is attributed to the long-range character of the strain-induced interactions, which cannot be readily captured by direct real-space methods. In contrast, the nonanalytic character of the strain-induced interaction, which is a direct consequence of the large Zener anisotropy factor of iron, is fully captured by the MET. For the determination of martensitic stability limits, we therefore calculate the chemical interactions solely atomistically, as defined by Eq. (1) while the strain-induced contribution is obtained within the MET [Eqs. (3) and (4)] using parameters from atomistic simulations.

By expressing the C-C interaction in Fourier space we can directly determine the equilibrium part of the phase diagram for Fe-C solid solutions by means of the static concentration waves method.<sup>13</sup> The main energetic parameters of this approach are  $\lambda_\sigma(\mathbf{k})$ —the eigenvalues of the interaction matrix  $\|V_{pq}^{\text{tot}}(\mathbf{k})\| = \|V_{pq}^{\text{si}}(\mathbf{k})\| + \|V_{pq}^{\text{ch}}(\mathbf{k})\|$ , where  $V^{\text{si}}(\mathbf{k})$  and  $V^{\text{ch}}(\mathbf{k})$  are the Fourier transforms of the strain-induced and chemical contributions to the C-C interactions and  $\sigma$  is the index of the eigenvalues. The global minimum of  $\lambda_\sigma(\mathbf{k})$  defines the configurational energy of the most stable phase, which we found to be  $\lambda_2(\mathbf{k}=0) = V_{11}^{\text{tot}}(0) - V_{12}^{\text{tot}}(0) = -10.773$  eV. This state corresponds to the stable ordered structure<sup>13</sup> (see Fig. 5) in which only one octahedral sublattice is occupied by C atoms. Such ordering results in tetragonal distortions of the host lattice along a well-defined orientation [001], as discussed above.

The critical (spinodal) temperature  $T_c$  of the order-disorder transition can be estimated within the mean-field theory and is related to the minimum of the eigenvalue  $\lambda_\sigma^{\min}(\mathbf{k})$  by

$$T_c = -\frac{c(1-c)\lambda_\sigma^{\min}(\mathbf{k}=0)}{k_B}. \quad (6)$$

Using the minimum eigenvalue  $\lambda_2(\mathbf{k}=0)$  of the interaction matrix, we calculated the temperature-dependent stability range of the disordered state with respect to the orientationally ordered tetragonally deformed phase as a function of the C concentration (Fig. 5). The disordered state consists of a random distribution of the C atoms over all octahedral interstices of the host Fe bcc lattice. In this case no orientational ordering occurs and the corresponding lattice has cubic symmetry. The critical C concentration at which an order-disorder transition occurs at room temperature is found to be 0.16 wt %, in good agreement with the only available experimental data (0.18 wt %).<sup>24</sup> We note that the predicted critical concentration was obtained using the 0 K elastic constants listed in Table I. In order to estimate whether finite temperature effects in the elastic constants affect the critical C concentration, we replaced the 0 K elastic constants by the temperature-dependent ones as obtained from experiment.<sup>31,32</sup> At room temperature, our results show a small increase of  $\sim 7\%$  in the critical concentration which brings it even closer to the experimentally observed value. A fully theoretical treatment of the temperature dependence is beyond the scope of the present study: as pointed out in Ref. 33, the temperature dependence of the elastic properties of  $\alpha$ -Fe is a consequence of magnetism and cannot be captured by the EAM potential used in this study.

For comparison we also studied the phase stability in a Fe-C solid solution when the chemical interactions are switched off. For this case the minimal eigenvalue of the interaction matrix is  $\lambda_1(\mathbf{k}=0) = V_{11}^{\text{tot}}(0) + 2V_{12}^{\text{tot}}(0) = -9.892$  eV. This value corresponds to a disordered phase, where all three interstitial sublattices are occupied with equal probability, and which is unstable with respect to a change in concentration.<sup>23</sup> This result clearly emphasizes the need to explicitly include repulsive chemical interactions: otherwise, the ordered (martensitic) state is not stable irrespective of temperature and C concentration.

In the predicted phase diagram in Fig. 5 the experimental eutectic isotherm and the solubility limit for C in bcc Fe have been indicated by thin lines to highlight the region where the martensitic order/disorder transformation can take place. The phase diagram suggests that there are two fundamentally different transformation mechanisms leading to the tetragonal states of Fe-C interstitial solid solutions. For C concentrations below  $c_{\max}$  a martensitic transformation involves a disordered intermediate phase, which necessitates atomistic diffusion to create the tetragonal noncubic lattice, whereas above  $c_{\max}$  a direct, (Bain-type) transformation from the austenitic fcc to the ordered (martensitic) phase takes place.<sup>6,7</sup> Below a certain temperature,  $T_d$ , the equilibration will be hindered due to the slow diffusion of the interstitial C atoms. Using the experimentally observed diffusion barrier of C in bcc Fe of 0.87 eV (Ref. 34) we estimate  $T_d$  to be 270 K. Below this temperature no transformation is expected. This temperature can be related to a concentration  $c_{\min} = 0.14$  wt % via the order/disorder temperature. This concentration sets a lower limit for the formation of the ordered (tetragonal) phase under realistic annealing (equilibration) conditions.

The above discussion of boundaries in the phase diagram (Fig. 5) correlates with well-known characteristics of steels.

For example, decreasing the carbon content in so-called mild steels softens them, i.e., increases their plasticity (see, e.g., Ref. 35). This may be attributed to the sparsity of martensite inclusions in the ferrite, which is the main constituent of these steels at C concentrations below  $\sim 0.16$  wt %. The onset of a diffusionless (Bain-type) transformation at  $c_{\max}$  is in good agreement with the experimentally observed lower limit of 0.5 wt % for the diffusionless transformation leading to Kurdjumov-Sachs<sup>36</sup> interfacial orientations. We note that this value will be a lower bound: taking temperature effects into account will soften the elastic constants and shift this value to higher concentrations.

#### IV. CONCLUSIONS

Combining microscopic elasticity theory with atomistic molecular static simulations provides an efficient approach to calculate structural and thermodynamic properties of intersti-

tial solid solutions. We cross-validated the results of both methods in real space and demonstrated the efficiency of the reciprocal-space microscopic elasticity theory for the description of long-range strain-induced interactions between interstitials. The application of this approach to the technologically important dilute Fe-C solid solution showed that both strain-induced and chemical interactions need to be taken into account for an accurate description of such systems. The approach employed in this study is straightforward to combine with *ab initio* methods and can be readily applied to other solid solutions.

#### ACKNOWLEDGMENTS

We would like to thank A. Dick and R. Kurta for fruitful discussions. Financial support through the “Triple-M-Max-Planck Initiative on Multiscale Materials Modeling of Condensed Matter” is gratefully acknowledged.

- 
- <sup>1</sup>W. L. Fink and E. D. Campbell, *Trans. Am. Soc. Steel Treat.* **9**, 717 (1926).
- <sup>2</sup>N. Seljakow, G. Kurdjumow, and N. Goodtzow, *Z. Phys.* **45**, 384 (1927).
- <sup>3</sup>V. A. Lobodyuk and E. I. Estrin, *Phys. Usp.* **48**, 713 (2005).
- <sup>4</sup>G. V. Kurdumoff and E. Kaminsky, *Nature (London)* **122**, 475 (1928).
- <sup>5</sup>G. V. Kurdjumov, *Metall. Trans. A* **7**, 999 (1976).
- <sup>6</sup>E. Bain, *Trans. AIME* **70**, 25 (1924).
- <sup>7</sup>G. V. Kurdjumov and G. Sachs, *Z. Phys.* **64**, 325 (1930).
- <sup>8</sup>L. I. Lyssak and V. E. Kanilchenko, *Fiz. Met. Metalloved.* **32**, 639 (1971).
- <sup>9</sup>G. V. Kurdjumov, L. K. Mikhailova, and A. G. Khachaturyan, *Sov. Phys. Dokl.* **18**, 159 (1974).
- <sup>10</sup>C. Zener, *Phys. Rev.* **74**, 639 (1948).
- <sup>11</sup>G. V. Kurdjumov and A. G. Khachaturyan, *Metall. Trans.* **3**, 1069 (1972).
- <sup>12</sup>G. V. Kurdjumov and A. G. Khachaturyan, *Acta Metall.* **23**, 1077 (1975).
- <sup>13</sup>A. G. Khachaturyan, *Theory of Structural Transformations in Solids* (Wiley, New York, 1983).
- <sup>14</sup>M. A. Krivoglaz, *X-Ray and Neutron Diffraction in Nonideal Crystals* (Springer-Verlag, Berlin, 1996).
- <sup>15</sup>H. E. Cook and D. de Fontaine, *Acta Metall.* **17**, 915 (1969).
- <sup>16</sup>D. W. Hoffman, *Acta Metall.* **18**, 819 (1970).
- <sup>17</sup>H. Kanzaki, *J. Phys. Chem. Solids* **2**, 2436 (1957).
- <sup>18</sup>M. Born and K. Huang, *Dynamical Theory of Crystal Lattices* (Clarendon, Oxford, 1998).
- <sup>19</sup>P. G. Winchell and M. Cohen, *Trans. Am. Soc. Met.* **55**, 347 (1962).
- <sup>20</sup>A. G. Khachaturyan and G. A. Shatalov, *Fiz. Met. Metalloved.* **32**, 5 (1971).
- <sup>21</sup>A. A. Smirnov, *Theory of Interstitial Alloys* (Nauka, Moscow, 1979).
- <sup>22</sup>Zhong Fan, Liu Xiao, Zhang Jinxiu, Kang Mokuang, and Guo Zhenqi, *Phys. Rev. B* **52**, 9979 (1995).
- <sup>23</sup>M. S. Blanter and A. G. Khachaturyan, *Phys. Status Solidi A* **51**, 291 (1979).
- <sup>24</sup>X. Liu, F. Zhong, J. Zhang, M. Zhang, M. Kang, and Z. Guo, *Phys. Rev. B* **52**, 9970 (1995).
- <sup>25</sup>J. Stadler, R. Mikulla, and H.-R. Trebin, *Int. J. Mod. Phys. C* **8**, 1131 (1997).
- <sup>26</sup>T. T. Lau, C. J. Först, X. Lin, J. D. Gale, S. Yip, and K. J. Van Vliet, *Phys. Rev. Lett.* **98**, 215501 (2007).
- <sup>27</sup>C. Domain, C. S. Becquart, and J. Foct, *Phys. Rev. B* **69**, 144112 (2004).
- <sup>28</sup>A. W. Cocharadt, G. Schoek, and H. Wiedersich, *Acta Metall.* **3**, 533 (1955).
- <sup>29</sup>M. S. Blanter and A. G. Khachaturyan, *Metall. Trans. A* **9**, 753 (1978).
- <sup>30</sup>C. S. Roberts, *Trans. AIME* **197**, 203 (1953).
- <sup>31</sup>J. A. Rayne and B. S. Chandrasekhar, *Phys. Rev.* **122**, 1714 (1961).
- <sup>32</sup>D. J. Dever, *J. Appl. Phys.* **43**, 3293 (1972).
- <sup>33</sup>S. L. Dudarev, R. Bullough, and P. M. Derlet, *Phys. Rev. Lett.* **100**, 135503 (2008).
- <sup>34</sup>C. A. Wert, *Phys. Rev.* **79**, 601 (1950).
- <sup>35</sup>M. F. Ashby and D. R. H. Jones, *Engineering Materials 2* (Pergamon Press, Oxford, 1992).
- <sup>36</sup>E. Macherauch and O. Vöhringer, *HTM, Haerterei-Tech. Mitt.* **41**, 71 (1986).